ISSN: 2454-1907
DOI: https://doi.org/10.29121/ijetmr.v4.i10.2017.114

IJETMR

International Journal of Engineering Technologies and Management Research
A Knowledge Repository

A QUANTUM CHEMICAL STUDY ON ELUCIDATION OF MOLECULAR STRUCTURE, ELECTRIC MOMENTS AND VIBRATIONAL ANALYSES OF BETA-DAMASCENONE AND ITS ISOMER- A COMPARATIVE STUDY

Amarendra Kumar [*1]
[*1] Department of Physics, Lucknow University, Lucknow-226007, India

Abstract:

A comparative, quantum chemical study on of energies, dipole moment and vibrational wavenumbers of trans- beta-Damascenone and cis-beta-Damscenone was carried out by using B3LYP methods with 6-311+G(d,p) and 6-311++G(d,p) basis sets. A complete vibrational analysis of both the compounds has been performed and assignments are made on the basis of potential energy distribution. The frontier orbitals and molecular electrostatic potential surface study has also been employed to understand the active sites of title compounds. The calculation of the IR spectra is not only important in order to confirm the validity of the simulations but it also allows additional insight into the molecular level of the system not accessible from experiment. Therefore, simulated IR and Raman spectra of the title compounds are also presented in this study. The structure activity relationship based on the study of frontier orbital gap, dipole moment data along with the molecular electrostatic potential map of the title compounds have been used to understand the active sites of the molecules.

Keywords: *Density Functional Theory; Frontier Orbital Energy Gap; Isomers; Damascenone.*

Cite This Article: Amarendra Kumar. (2017). "A QUANTUM CHEMICAL STUDY ON ELUCIDATION OF MOLECULAR STRUCTURE, ELECTRIC MOMENTS AND VIBRATIONAL ANALYSES OF BETA-DAMASCENONE AND ITS ISOMER- A COMPARATIVE STUDY." *International Journal of Engineering Technologies and Management Research*, 4(10), 123-136. DOI: https://doi.org/10.29121/ijetmr.v4.i10.2017.114.

1. Introduction

Damascenones are a series of closely related chemical compounds that are components of a variety of essential oils. The damascenones are categorized under rose ketones, which also include ionones. β Damascenone provides the aroma of roses, despite its very low concentration, and is an essential fragrance chemical used in perfumery[1]. The damascenones are derived from the degradation of carotenoids [2]. In 2008, (E) β-damascenone was identified as a primary and essential odorant in Kentucky Bourbon whisky and tea infusions indicating the importance of these compounds in the overall aroma of these products [3, 4]. Damascenone is considered to be an important impact aroma component in grape juice and wine (Naiker & Allen, 1996; Kotseridis et al., 1999; Kotseridis & Baumes, 2000; Waldner & Marais, 2002). It has a complex

ISSN: 2454-1907
DOI: 10.5281/zenodo.1051048

aroma which has been described as reminiscent of exotic flowers with fruit and berry undertones (Ohloff, 1978; Naiker & Allen, 1996), and also as sweet, raisin-like (Simpson & Millar, 1984), honey-like, iononelike and cooked quince-like (Kotseridis et al., 1999). Damascenone was first identified in grapes and wine by Schreier & Drawert (1974) and mechanisms for its formation from the carotenoid neoxanthin were proposed by Skouroumounis & Sefton (2001). Damascenone occurs in Pinotage, Shiraz and Cabernet Sauvignon wines well above the threshold values reported by most researchers [5-8].

The aim of the present communication is to investigate the molecular structural, vibrational and energetic data analysis of the molecules under study, in gas phase, due to their biological and industrial importance. The structure and the ground state energy of the molecules under investigation has been analyzed employing DFT/B3LYP level. In order to obtain a more complete description of molecular motion, vibrational frequency calculations have been carried out at the DFT level. The vibrational analysis also yields the detailed information about the intra molecular vibrations in the molecular fingerprint region. The reported geometries, molecular properties such as equilibrium energy, dipole moment and vibrational frequencies along with the electrostatic potential maps, have also been used to understand the activity of the molecules.

2. Computational Methods

The DFT calculations [9] of the title molecules under investigation have been performed by employing Becke's three parameter hybrid exchange functionals [10] with Lee–Yang–Parr functional (B3LYP) [11,12] method using the Gaussian 03 program [13]. The vibrational frequencies are also calculated and scaled down by the appropriate factor [14]. The vibrational frequency assignments have been carried out by combining the results of the Gaussview 5.0.8 program [15], symmetry considerations and the VEDA 4 program [16].

3. Result and Discussion

3.1. Molecular Geometry Optimization and Energies

The structure of trans β-damascenone and cis-β-damascenone has been investigated in order to assess the difference and similarities in the properties of these two isomers. The equilibrium geometry optimization for both the molecules has been achieved by energy minimization, using DFT at the B3LYP level, employing the basis set 6-311++G (d, p). The optimized geometry of both molecules under study are confirmed to be located at the local true minima on potential energy surface, as the calculated vibrational spectra has no imaginary frequency. The optimized molecular structures thus obtained together with the numbering scheme of the atoms are shown in Fig. 1. The optimized geometrical parameters of trans-β-damascenone and cis-β-damascenone have been given in Table1 and Table 2 respectively. In case of both the compounds, two C-C double bonds of six membered ring have values 1.338 and 1.3567 Å/ 1.33782 and 1.35723 Å respectively; and other C-C bond lengths of six membered ring are calculated between the range (1.468 Å -1.547 Å). The C=O bond length in both the molecules equal to 1.22 Å are also consistent with the standard C=O bond length (1.22 Å) [17, 18]. The six membered ring endocyclic C–C–C angles in trans-β-damascenone/cis-β-damascenone are found to be varying in

ISSN: 2454-1907
DOI: 10.5281/zenodo.1051048

the range (108.9-121.5)/ (109.0-121.5) degree. The skeleton of both the molecules is not strictly planar, the carbonyl groups deviate from the plane of five membered rings.

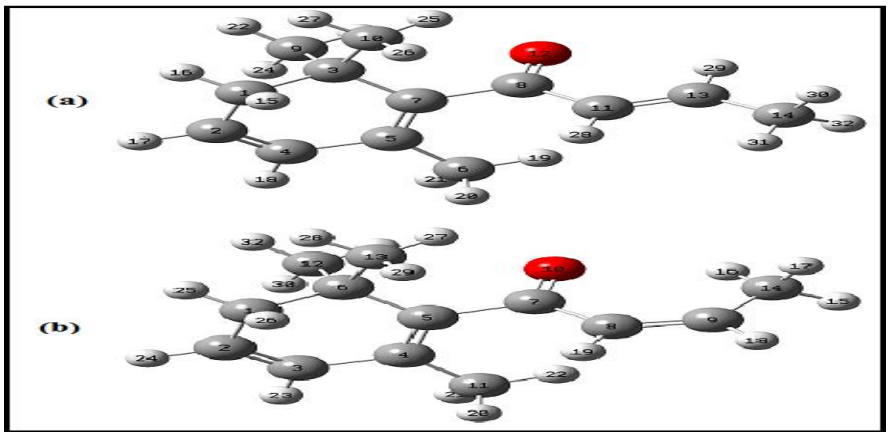

Figure 1: 3D optimized structures along with numbering scheme of (a) trans- β-damascenone (b) cis- β-damascenone

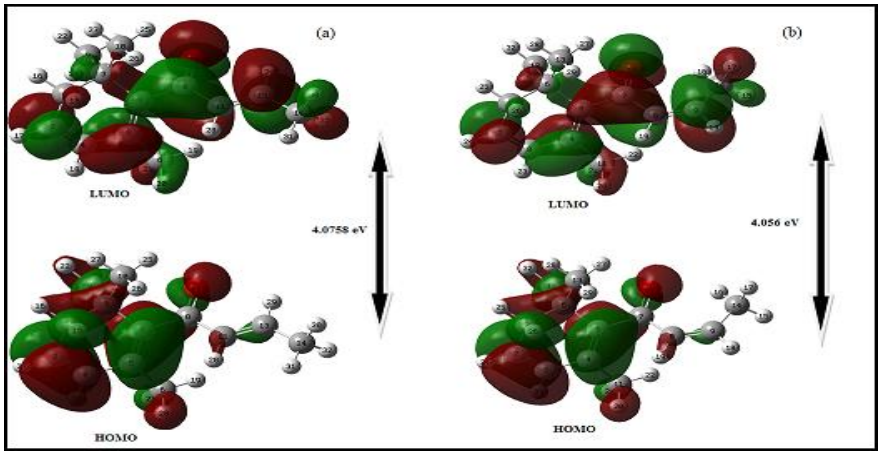

Figure 2: Patterns of the principle highest occupied and lowest unoccupied molecular orbitals of (a) trans- β-damascenone and (b) cis- β-damascenone obtained with B3LYP/6-311++G(d,p)

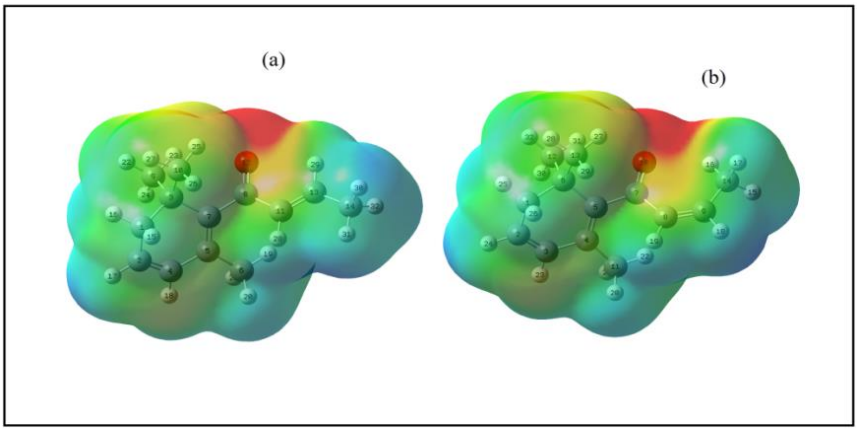

Figure 3: MESP surface of (a) trans- β-damascenone and (b) cis- β-damascenone obtained with B3LYP/6-311++G(d,p)

ISSN: 2454-1907
DOI: 10.5281/zenodo.1051048

Table 1: Optimized parameters of trans- and cis- β-damascenone at DFT/B3LYP/6311++G (d, p)

Parameter	trans-β-damascenone	cis-β-damascenone
ZPE (kcal mol^{-1})	172.729	172.902
E (kcal mol^{-1})	182.352	182.498
C_v (cal mol^{-1} K^{-1})	58.047	57.830
S (cal mol-1 K^{-1})	122.083	122.482
G (kcal mol^{-1})	146.544	146.571
H (kcal mol^{-1})	157.416	175.559
Energy Gap (eV)	4.0758	4.056
Electric Dipole Moment (Debye)	2.9105	2.4711

3.2. Electronic Properties

The most important orbitals in a molecules are the frontier molecular orbitals, called highest occupied molecular orbital (HOMO) and lowest unoccupied molecular orbital (LUMO). These orbitals determine the way the molecule interacts with other species. The frontier orbital gap helps characterize the chemical reactivity and kinetic stability of the molecule. A molecule with a small frontier orbital gap is more polarizable and is generally associated with a high chemical reactivity, low kinetic stability and is also termed as soft molecule [19]. The lower value for frontier orbital gap in case of cis conformer of damascenone than trans conformer of damascenone makes it more reactive and less stable (refer to Table 1). The HOMO is the orbital that primarily acts as an electron donor and the LUMO is the orbital that largely acts as the electron acceptor. The 3D plots of the frontier orbitals HOMO and LUMO and the molecular electrostatic potential (MESP) map for both molecules are shown in Fig. 2 and Fig.3 respectively. It can be seen from the figure that, the HOMO is distributed uniformly in both the compounds over six membered ring and carbonyl group and the LUMO is found to spread over entire molecule except the atom C (10) in both the molecules. All the HOMO and LUMO have nodes. The nodes in each HOMO and LUMO are placed symmetrically. The MESP which is a plot of electrostatic potential mapped onto the constant electron density surface is shown in Fig. 3. The resulting surface simultaneously displays electrostatic potential value over the molecular shape and size. The MESP map for both the isomers clearly suggests that the carbonyl oxygen atoms (dark red) have maximum negative and probable site for nucleophillic attack, and the hydrogen atoms attached to the six membered ring and that attached to the carbon chain bear the most positive charge (blue region).The dipole moment in a molecule is another important electronic property that results from non-uniform distribution of charges on the various atoms in a molecule. It is mainly used to study the intermolecular interactions involving the van der Waal type dipole–dipole forces, etc., because larger the dipole moment, stronger will be the intermolecular interactions. Here large value of dipole moment in cis- isomer in comparison to trans isomer makes cis-β-damascenone more polar than trans-β-damascenone molecule. The calculated frontier orbital gap, dipole moment values for both the molecules are also given in Table 1.

ISSN: 2454-1907
DOI: 10.5281/zenodo.1051048

Table 2: The optimized geometric parameters of trans-β-damascenone, bond lengths in angstrom (Å), bond angles and selected dihedral angles (in degrees)

Parameter	Theoretical Value	Parameter	Theoretical Value
C1-C6	1.5484	C6-C12	1.5475
C1-H25	1.0949	C6-C13	1.5417
C1-H26	1.1015	C7-C8	1.489
C2-C3	1.3378	C7-O10	1.2264
C2-H24	1.0855	C8-C9	1.3444
C3-C4	1.4691	C8-H19	1.085
C3-H23	1.0859	C9-C14	1.4955
C4-C5	1.3572	C6-C12	1.5475
C2-C1-C3	113.3857	C3-C7-C8	117.131
C2-C1-H15	108.2863	C5-C7-C8	121.943
C2-C1-H16	110.8118	C7-C8-C11	117.9045
C3-C1-H15	109.2369	C7-C8-C12	120.6967
C3-C1-H16	108.8613	C3-C9-H22	110.0564
H15-C1-H16	105.9842	C3-C9-H23	110.1925
C1-C2-C4	119.827	C3-C9-H24	111.2987
C1-C2-H17	119.3578	H22-C9-23	108.5944
C4-C2-H17	120.7655	H22-C9-24	108.1384
C1-C3-C7	108.9993	H23-C9-24	108.4863
C1-C3-C9	110.1104	C3-C10-H25	111.6605
C1-C3-C10	107.7047	C3-C10-H26	111.3117
C7-C3-C9	108.7887	C3-C10-H27	109.6579
C7-C3-C10	112.2938	H25-C10-H26	108.4208
C9-C3-C10	108.9325	H25-C10-H27	107.953
C2-C4-C5	121.5417	H26-C10-H27	107.6965
C2-C4-H18	120.6764	C8-C11-C13	121.6043
C5-C4-H18	117.7568	C8-C11-H28	117.6593
C4-C5-C6	114.7331	C13-C11-H28	120.6919
C4-C5-C7	119.8657	C11-C13-C14	125.4881
C6-C5-C7	125.3005	C11-C13-H29	117.2008
C5-C6-H19	113.7845	C14-C13-H29	117.3106
C5-C6-H20	110.8046	C13-C14-H30	110.5715
C5-C6-H21	109.3213	C13-C14-H31	112.1866
H19-C6-H20	108.4883	C13-C14-H32	110.594
H19-C6-H21	107.5759	H30-C14-H31	108.4995
H20-C6-H21	106.5696	H30-C14-H32	106.2517
C3-C7-C5	120.5009	H31-C14-H32	108.5273
C3-C1-C2-C4	30.9339	C1-C3-C9-H22	61.3344
C3-C1-C2-H17	-151.6101	C1-C3-C9-H23	-178.933
H15-C1-C2-C4	-90.4624	C1-C3-C9-H24	-58.5359
H15-C1-C2-H17	86.9935	C7-C3-C9-C22	-179.274
H16-C1-C2-C4	153.6971	C7-C3-C9-C23	-59.5413

ISSN: 2454-1907
DOI: 10.5281/zenodo.1051048

H16-C1-C2-H17	-28.8469	C7-C3-C9-C24	60.8558
C2-C1-C3-C7	-44.7632	C10-C3-C9-H22	-56.5684
C2-C1-C3-C9	74.5002	C10-C3-C9-H23	63.1642
C2-C1-C3-C10	-166.8415	C10-C3-C9-H24	-176.4387
H15-C1-C3-C7	76.0985	C1-C3-C10-H25	-174.2975
H15-C1-C3-C9	-164.6382	C1-C3-C10-H26	64.3773
H15-C1-C3-C10	-45.9798	C1-C3-C10-H27	-54.6902
H16-C1-C3-C7	-168.5976	C7-C3-C10-H25	65.6867
H16-C1-C3-C9	-49.3343	C7-C3-C10-H26	-55.6385
H16-C1-C3-C10	69.3241	C7-C3-C10-H27	-174.7059
C1-C2-C4-C5	-0.1138	C9-C3-C10-H25	-54.8868
C1-C2-C4-H18	178.0234	C9-C3-C10-H26	-176.212
H17-C2-C4-C5	-177.5333	C9-C3-C10-H27	64.7205
H17-C2-C4-H18	0.6039	C21-C4-C5-C6	169.0823
C1-C3-C7-C5	33.176	C21-C4-C5-C7	-14.3753
C1-C3-C7-C8	-154.1628	H18-C4-C5-C6	-9.1074
C9-C3-C7-C5	-86.9065	H18-C4-C5-C7	167.4351
C9-C3-C7-C8	85.7547	C4-C5-C6-H19	173.4889
C10-C3-C7-C5	152.4369	C4-C5-C6-H20	-63.9517
C10-C3-C7-C8	-34.9019	C4-C5-C6-H21	53.2096

Table 3: The optimized geometric parameters of cis-β-damascenone, bond lengths in angstrom (Å), bond angles and selected dihedral angles (in degrees)

Parameter	**Theoretical Value**	**Parameter**	**Theoretical Value**
C1-C2	1.4995	C8-C9	1.3444
C1-C6	1.5484	C8-H19	1.085
C1-H25	1.0949	C9-C14	1.4955
C1-H26	1.1015	C9-H18	1.0894
C2-C3	1.3378	C11-H20	1.0961
C2-H24	1.0855	C11-H21	1.0956
C3-C4	1.4691	C11-H22	1.0875
C3-H23	1.0859	C12-H30	1.0927
C4-C5	1.3572	C12-H31	1.0904
C4-C11	1.5109	C12-H32	1.0958
C5-C6	1.5462	C13-H27	1.09
C5-C7	1.5024	C13-H28	1.0944
C6-C12	1.5475	C13-H29	1.0946
C6-C13	1.5417	C14-H15	1.0953
C7-C8	1.489	C14-H16	1.0864
C7-O10	1.2264	C14-H17	1.0975
C2-C1-C6	113.3852	C6-C12-H32	110.0234
C2-C1-H25	110.8013	H30-C12-H31	108.5207
C2-C1-H26	108.2737	H30-C12-H32	108.1446
C6-C1-H25	108.8644	H31-C12-H32	108.6057

ISSN: 2454-1907
DOI: 10.5281/zenodo.1051048

C6-C1-H26	109.2378	C6-C13-H27	111.7353
H25-C1-H26	106.0054	C6-C13-H28	109.6007
C1-C2-C3	119.7932	C6-C13-H29	111.3068
C1-C2-H24	119.3726	H27-C13-H28	107.9429
C3-C2-H24	120.7825	H27-C13-H29	108.431
C2-C3-C4	121.5795	H28-C13-H29	107.681
C2-C3-H23	120.6686	C9-C14-H15	109.8897
C4-C3-H23	117.7265	C9-C14-H16	112.57
C3-C4-C5	119.9126	C9-C14-H17	109.5782
C3-C4-C11	114.5106	H15-C14-H16	110.3332
C5-C4-H11	125.4852	H15-C14-H17	106.2706
C4-C5-C6	120.3794	H16-C14-H17	107.9835
C4-C5-C7	122.0568	C6-C1-C2-C3	30.9982
C6-C5-C7	117.0796	C6-C1-C2-H24	-151.596
C1-C6-C5	109.026	H25-C1-C2-C3	153.7571
C1-C6-C12	110.0442	H26-C1-C2-C3	-90.39
C1-C6-C13	107.5559	H26-C1-C2-H24	87.0158
C5-C6-C12	108.894	C2-C1-C6-C5	-44.8468
C5-C6-C13	112.3588	C2-C1-C6-C12	74.5219
C12-C6-C13	108.9452	C2-C1-C6-C13	-166.9294
C5-C7-C8	117.5182	H25-C1-C6-C5	-168.6696
C5-C7-O10	120.1182	H25-C1-C6-C12	-49.301
C8-C7-O10	122.2502	H25-C1-C6-C13	69.2477
C7-C8-C9	126.6252	H26-C1-C6-C5	75.9991
C7-C8-H19	115.4207	H26-C1-C6-C12	-164.6323
C9-C8-H19	117.9448	H26-C1-C6-C13	-46.0835
C8-C9-C14	129.0032	C1-C2-C3-C4	-0.1379
C8-C9-H18	114.9624	C1-C2-C3-H23	177.9841
C4-C11-H20	110.7055	H24-C2-C3-C4	-177.5064
C4-C11-H21	109.291	H24-C2-C3-H23	0.6156
C4-C11-H22	113.8424	C2-C3-C4-C5	-14.4022
H20-C11-H21	106.5797	C2-C3-C4-C11	168.8889
H20-C11-H22	108.3863	H23-C3-C4-C5	167.4226
H21-C11-H22	107.744		
C6-C12-H30	111.3034		
C6-C12-H31	110.1706		

3.3. Vibrational Analysis

The optimized molecular structure belongs to the C1 point group as it does not display any special symmetry. The calculated IR spectra of both the compounds have been given in Fig. 4. The overestimation of the vibrational wavenumbers in ab-initio and DFT methods are corrected either by computing anharmonic correlations explicitly or by introducing a scaled field [20], even directly scaling the calculated wavenumbers with proper factor. The vibrational wavenumbers are calibrated accordingly with the scaling factor of 0.9679 for DFT at B3LYP

ISSN: 2454-1907
DOI: 10.5281/zenodo.1051048

[21]. The vibrational assignments have been done on the basis of relative intensities, line shape, the VEDA 4 program and the animation option of Gaussview 5. The calculated and scaled wavenumber of trans β-damascenone and cis-β-damascenone are given in Table 5 and Table respectively. The calculated vibrational spectra of both the molecules have been divided in two regions; a low wavenumber fingerprint region (<2000 cm-1) and a high wavenumber functional group region (4000- 2000 cm-1). A total of 90 (3N-6) normal modes of vibrations have been calculated for for trans-β-damascenone and cis-β-damascenone and given alongwith potential energy distribution in table 4 and Table 5 respectively.

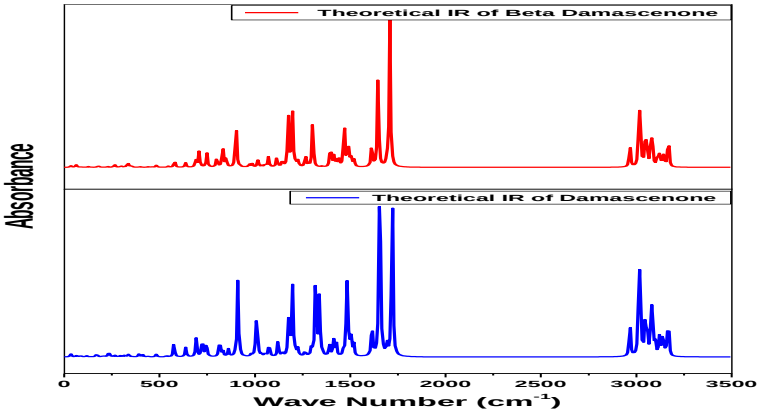

Figure 4: Theoretical FTIR Spectra of trans- β-damascenone and cis- β-damascenone

Table 4: Vibrational analysis of prominent modes of trans-β-Damascenone at the B3LYP/6-11++G (d, p) level

IR frequency (in cm^{-1})	Scaled Frequency (in cm^{-1})	Assignment
3168.09	3063	$\nu_{s[(C2-H17)(64) + (C4-H18)(34)]}$
3161.58	3057	$\nu_{(C11-H28)(96)}$
3145.20	3041	$\nu_{as[(C2-H17)(35) + (C4-H18)(65)]}$
3142.20	3038	$\nu_{(C13-H29)(93)}$
3135.13	3031	$\nu_{[(C6-H19)(90)]}$
3121.68	3018	$\nu_{s[(C9-H23)(41) + (C10-H25)(43)]}$
3118.08	3015	$\nu_{as[(C9-H23)(38) + (C10-H25)(44)]}$
3098.76	2996	$\nu_{[(C14-H31)(79)]}$
3084.15	2982	$\nu_{as[(C9-H22)(29) + (C9-H24)(60)]}$
3077.67	2976	$\nu_{as[(C10-H26)(43) + (C10-H27)(53)]}$
3055.92	2955	$\nu_{as[(C6-H20)(40) + (C6-H21)(60)]}$
3054.96	2954	$\nu_{as[(C14-H30)(51) + (C14-H32)(49)]}$
3045.29	2945	$\nu_{[(C1-H16)(95)]}$
3023.22	2923	$\nu_{s[(C10-H26)(44) + (C10-H27)(35)]}$
3016.44	2917	$\nu_{s[(C9-H22)(61) + (C9-H24)(17)]}$
3014.83	2915	$\nu_{s[(C6-H20)(55) + (C6-H21)(35)]}$
3012.78	2913	$\nu_{s[(C14-H30)(40) + (C14-H31)(17) + (C14-H32)(42)]}$
2966.10	2868	$\nu_{[(C1-H15)(96)]}$

ISSN: 2454-1907
DOI: 10.5281/zenodo.1051048

1720.46	1663	ν_{as}[(O12-C8)(45) + (C13-C11)(32)]
1692.57	1637	ν[(C2-C4)(23)]
1654.97	1600	ν_{s}[(O12-C8)(44) + (C13-C11)(35)]
1613.84	1560	ν[(C2-C4)(40)]+σ[(C3-C7-C5)(17)]
1518.08	1468	σ[(H25-C10-H27)(17)+ (H24-C9-H23)(16) +(H26-C10-H25)(33)]
1504.40	1455	σ[(H25-C10-H27)(28)+(H27-C10-H26)(21)]
1498.50	1449	σ[(H23-C9-H22)(31)]+ τ [(H24-C9-H23)(16)]
1492.61	1443	σ[(H19-C6-H21)(54)+ (H21-C6-H20)(20)] + τ_i [(H21-C6-C5-C7)(15)]
1484.20	1435	σ[(H22-C9-H24)(28)+(H27-C10-H26)(16)]
1483.69	1435	σ[(H20-C6-H10)(48)+(H21-C6-H20)(11)]
1483.26	1434	σ[(H30-C14-H32)(30)]+τ[(H31-C14-H30)(22) +(H32-C14-H31)(15)]
1476.86	1428	σ[(H31-C14-H30(37)+(H32-C14-H31)(43)]
1464.50	1416	σ[(H16-C1-H15)(77)
1427.00	1380	σ[(H17-C2-C4)(34)+ (H18-C4-C2)(41)]
1415.98	1369	ω[(H21-C6-H20)(25)]
1412.96	1366	ω[(H21-C6-H20)(24)]
1408.91	1362	ω[(H30-C14-H32)(47)+ (H31-C14-H30)(22) +(H32-C14-H31)(23)]
1390.93	1345	ω[(H23-C9-H22)(23)+ (H22-C9-H24)(21) +(H24-C9-H23)(24)]
1353.99	1309	τ_i [(H15-C1-C2-C4)(24)+(H16-C1-C2-C4)(33)]
1338.45	1294	σ[(H28-C11-C13)(51)]
1318.55	1275	σ[(H29-C13-C14)(61)]
1297.03	1254	τ [(H15-C1-C2)(13)]
1263.03	1221	σ[(H15-C1-C2)(23)]
1225.90	1185	σ[(H18-C4-C2)(25)]
1212.94	1173	ν[(C10-C3)(17)]+ τ_i [(H22-C9-C3-C1)(21)]
1178.26	1139	σ[(H17-C2-C4)(26)]
1144.90	1107	σ[(H15-C1-C2)(32)]
1121.23	1084	ν[(C14-C13)(29)]
1075.61	1040	τ_i [(H29-C13-C11-C8)(28)+(H31-C14-C13-C11)(41)]
1052.98	1018	ω[(H19-C6-H21)(32)]+ τ_o[(H19-C6-C5-C7)(47)]
1034.49	1000	τ_i [(H24-C9-C3-C1)(19)+(H26-C10-C3-C1)(21)]
1015.92	982	ν[(C1-C2)(28)]
1008.99	976	τ_i [(H28-C11-C13-C14)(49)+(H29-C13-C11-C8)(26)]
1003.62	970	ν[(C11-C8)(20)]
990.60	958	τ_i [(H17-C2-C4-C5)(32)+(H18-C4C2-C1)]
947.69	916	ν[(C10-C3)(17)]+ τ_i [(H23-C9-C3-C1)(16)]
920.56	890	ν_{s}[(C1-C2)(15) + (C10-C3)(15)]
910.67	880	ν[(C14-C13)(18)]+ τ_i [(H30-C14-C13-C11)(15)]
861.45	833	τ_i [(H28-C11-C13-C14)(16)]+ τ_o [(H28-C11-C13-C14)(28)]
745.07	720	τ_i [(H17-C2-C4-C5)(32)]
724.52	701	τ_o[(O12-C7-C11-C8)(24)]
692.77	670	σ[(C2-C4-C5)(61)]
439.44	425	σ[(C6-C5-C4)(21)] $+\tau_o$[(C10-C1-C7-C3)(22)]
412.05	398	σ[(C14-C13-C11)(33)]

ISSN: 2454-1907
DOI: 10.5281/zenodo.1051048

391.65	379	ω[(C10-C3-C9)(59)]
359.92	348	σ[(C6-C5-C4)(22)]
338.17	327	τ_o[(C6-C7-C4-C5)(21)]
316.43	306	σ[(C9-C3-C7)(20)]
283.89	274	τ_i [(H25-C10-C3-C1)(19)+ (H26-C10-C3-C1)(22)]+ (H27-C10-C3-C1)(17)]
265.63	257	σ[(C3-C7-C5)(15)]
253.36	245	τ_i [(H23-C9-C3-C1)(16)+ (H24-C9-C3-C1)(19)]
234.63	227	σ[(C8-C7-C5)(20)]
207.94	201	τ_i [(H32-C14-C13-C11)(19)+ τ_o[(C8-C3-C5-C7)(15)]
198.94	192	τ_i [(C14-C13-C11-C8)(53)]
171.43	166	σ[(C8-C7-C5)(17)]+ τ_i [(C14-C13-C11-C8)(18)]+ τ_o[(O12-C7-C11-C8)(17)]
166.08	160	τ_i [(H19-C6-C5-C7)(19)+ (H20-C6-C5-C7)(17)]
136.61	132	τ_i [(C2-C4-C5-C7)(31)]
87.90	85	τ_i [(C13-C11-C8-C7)(36)+ (C11-C8-C7-C3)(21)]
65.10	63	τ_i [(C3-C7-C5-C4)(24)]+ τ_o[(C8-C3-C5-C7)(24)]
34.43	33	τ_i [(C13-C11-C8-C7)(31)+ (C11-C8-C7-C3)(21)]

Table 5: Vibrational analysis of prominent modes of cis-β-Damascenone at the B3LYP/6-11++G (d, p) level

IR frequency (in cm^{-1})	**Scaled IR Frequency (in cm^{-1})**	**Assignment**
3168.50	3064	ν_s[(C2-H24)(61) + (C3-H23)(38)]
3166.51	3062	ν[(C8-H19)(77)]
3161.82	3057	ν_{as}[(C8-H19)(17)+ (C14-H16)(76)]
3146.06	3042	ν_{as}[(C2-H24)(37) + (C3-H23)(60)]
3141.17	3037	ν[(C11-H22)(91)]
3123.58	3020	ν_s[(C12-H31)(60)+ (C13-H27)(24)]
3120.30	3017	ν_{as}[(C12-H31)(22)+ (C13-H27)(63)]
3111.40	3009	ν[(C31-H18)(92)]
3084.15	2982	ν_{as}[(C12-H30)(62)+ (C12-H32)(29)]
3076.66	2975	ν_{as}[(C13-H28)(52)+ (C13-H29)(44)]
3055.95	2955	ν_{as}[(C11-H20)(41)+ (C11-H21)(58)]
3052.46	2952	ν_{as}[(C14-H15)(68)+ (C14-H17)(30)]
3045.25	2945	ν[(C1-H25)(95)]
3023.07	2923	ν_s[(C13-H28)(34)+ (C13-H29)(41)]
3017.07	2917	ν_s[(C12-H30)(17)+ (C12-H32)(58)]
3015.39	2916	ν_s[(C11-H20)(54)+ (C11-H21)(38)]
3012.00	2912	ν_s[(C14-H15)(27)+ (C14-H17)(68)]
2966.28	2868	ν[(C1-H26)(96)]
1707.77	1651	ν_{as}[(O10-C7)(50)+ (C9-C8)(50)]
1692.85	1637	ν_{as}[(C2-C3)(38)+ (C5-C4)(24)]
1645.87	1591	ν_s[(O10-C7)(37)+ (C9-C8)(40)]
1612.73	1559	ν[(C2-C3)(27)]
1520.59	1470	σ[(H31-C12-H30)(21)+ (H27-C13-H29)(28)]+ρ[(H28-C13-H27)(15)]

ISSN: 2454-1907
DOI: 10.5281/zenodo.1051048

1506.47	1457	σ[(H31-C12-H30)(18)+ (H28-C13-H27)(31)]+ τ [(H29-C13-H28)(12)]
1500.40	1451	σ[(H32-C12-H31)(29)+ (H29-C13-H28)(18)]
1490.57	1441	σ[(H22-C11-H21)(57)+ (H21-C11-H20)(18)]
1489.54	1440	ρ [(H16-C14-H15)(20)]+ σ [(H17-C14-H16)(52)]
1485.99	1437	σ[(H20-C11-H22)(55)]+ ρ [(H21-C11-H20)(12)]
1485.50	1436	ρ [(H30-C12-H32)(28)]+ σ [(H29-C13-H28)(19)]
1468.25	1420	σ[(H16-C14-H15)(38)+ (H15-C14-H17)(23)]
1465.07	1417	σ[(H26-C1-H25)(76)]
1440.58	1393	σ[(H19-C8-C9)(34)+ (H18-C9-H8)(26)]
1427.19	1380	σ[(H24-C2-C1)(25)+ (H23-C3-H2)(38)]
1416.32	1369	σ[(H21-C11-H20)(22)]
1413.04	1366	σ[(H21-C11-H20)(25)]
1398.77	1352	ω[(H16-C14-H15)(21)+(H15-C14-H17)(38)+ (H17-C14-H16)(24)]
1392.78	1347	ω[(H31-C12-H30)(22)+(H30-C12-H32)(19)+ (H32-C12-H31)(21)]
1352.97	1308	τ_i [(H25-C1-C2-C3)(28)+ (H26-C1-C2-C3)(27)]
1302.94	1260	σ[(C6-C5-C4)(10)]
1280.70	1238	σ[(H19-C8-C9)(31)+ (H18-C9-C8)(33)]
1265.14	1223	σ[(H25-C1-C2)(16)]+ τ_i [(H26-C1-C2-C3)(20)]
1226.60	1186	σ[(H23-C3-C2)(28)]
1213.84	1174	ν[(C13-C6)(17)]+ τ_i [(H32-C12-C6-C1)(18)]
1175.28	1136	ν[(C7-C5)(16)]+ σ[(H24-C2-C1)(23)]
1144.27	1106	σ [(H25-C1-C2)(25)]
1114.94	1078	τ_i [(H15-C14-C9-C8)(15)]+ τ_O[(H17-C14-C9-C8)(17)]
1072.66	1037	τ_O[(H18-C9-C8-C7)(15)+ (H16-C14-C9-C8)(27)] + τ_i [(C14-C9-C8-C7)(15)]
1071.35	1036	τ_i [(H16-C14-C9-C8)(27)]
1053.49	1019	τ_O[(H22-C11-C4-C3)(23)]+ τ_i [(H21-C11-C4-C3)(27)]
1036.43	1002	τ_i [(H30-C12-C6-C1)(20)+ (H29-C13-C6-C1)(20)]
1016.73	983	ν_{as}[(C1-C2)(35)]
1014.66	981	τ_O[(H19-C8-C9-C14)(46)+ (H18-C9-C8-C7)(16)]
992.00	959	τ_O [(H24-C2-C3-C4)(32)+ (H23-C2-C3-C1)(43)]
985.73	953	σ[(C2-C3-C4)(11)]
971.02	939	ν_{as}[(C8-C7)(16)]+ ν_{as}[(C14-C9)(15)]
949.52	918	ν_{as}[(C13-C6)(17)]+ τ_i [(H31-C12-C6-C1)(15)]
901.27	871	ν_{as}[(C14-C9)(42)]
898.94	869	ν_{as}[(C12-C6)(16)]
849.08	821	ν_{as}[(C12-C6)(16)]+ τ_O[(HO10-C8-C5-C7)(18)]
831.10	803	σ[(O10-C7-C8)(24)]
800.59	774	τ_i [(H18-C9-C8-C7)(18)]+ τ_O [(O10-C8-C5-C7)(16)]*
748.14	723	τ_i [(H24-C2-C3-C4)(26)]

ISSN: 2454-1907
DOI: 10.5281/zenodo.1051048

707.81	684	σ[(C1-C2-C3)(18)]
690.79	668	τ_i [(H19-C8-C9-C14)(24)]
578.49	559	τ_i [(C2-C3-C4-C5)(15)]
459.49	444	σ[(C14-C9-C8)(29)]
441.02	426	σ[(C11-C4-C3)(16)]+ τ_O [(C13-C1-C5-C6)(20)]
396.45	383	σ[(C13-C6-C12)(23)]+ τ_O [(C13-C1-C5-C6)(22)]
347.25	336	σ[(C11-C4-C3)(20)]+ τ_i [(C14-C9-C8-C7)(22)]
316.01	305	σ[(C13-C6-C12)(24)]
290.19	281	τ_i [(H31-C12-C6-C1)(19)]
257.44	249	τ_i [(H30-C12-C6-C1)(18)]
228.61	221	σ[(C14-C9-C8)(16)]
182.56	176	σ[(C7-C5-C4)(17)]
138.64	134	τ_O [(C11-C3-C5-C4)(16)]
125.99	122	τ_i [(H29-C13-C6-C1)(20)]
86.78	84	τ_i [(H16-C14-C9-C8)(22)]+ τ_i [(H15-C14-C9-C8)(17)]+ τ_i [(H17-C14-C9-C8)(28)]
73.21	71	σ[(C8-C7-C5)(22)]+ τ_O [(C7-C6-C4-C5)(17)]
61.94	60	τ_i [(C8-C7-C5-C6)(68)]
35.03	34	τ_i [(C9-C8-C7-C5)(76)]+ τ_i [(C8-C7-C5-C6)(16)]

3.3.1. C-C and C-H Vibrations

C-C stretching wavenumbers are observed as mixed modes in the range 1500 cm-1 to 1100 cm-1 and agree well with the general appearance of C-H and C-C stretching modes. C-C stretches are calculated to be (1490-1078) cm-1 trans-β-damascenone and (1518-1296) cm-1 for cis- β-damascenone. The C-H stretching vibrations for both the compounds are calculated in the range 3000 cm-1 -3200 cm-1.

3.3.2. Ring Vibrations

The six membered ring spectral region predominantly involves the C–H, C–C and C=C stretching, and C–C–C as well as H–C–C-bending vibrations. The bands due to the ring C–H-stretching vibrations were observed as a group of partially overlapping absorptions in the region 3110–3069 cm-1 with more than 90% potential energy contribution. Vibrations involving C–H in-plane bending are found in the region 1600–825 cm-1. The computed wavenumbers at 1017 cm-1 are identified as the trigonal ring bending and 1022 cm-1 as ring breathing modes respectively.

4. Conclusions

The present study on trans β-damascenone and cis-β-damascenone, comprised of equilibrium geometries optimization and the calculation of molecular ground state properties at DFT/6-311++G (d, p) level. In general, a slight change in the calculated optimized parameters in cis

ISSN: 2454-1907
DOI: 10.5281/zenodo.1051048

isomer has been observed. Theoretical IR spectra and normal mode analysis of title compounds has also been done and compared. The lower value of frontier orbital gap makes cis-β-damascenone more polarizable hence more reactive than trans β-damascenone. The structure activity relationship based on the study of frontier orbital gap, dipole moment data along with the molecular electrostatic potential map of trans β-damascenone and cis-β-damascenone, have been used to understand the active sites of the molecules under study.

References

[1] Rose (Rosa damascena) (http://www.leffingwell.com/rose.htm), John C. Leffingwell
[2] The Synthesis of Damascenone and beta Damascone and the possible mechanism of their formation from carotenoids". Helvetica Chimica Acta 56 (5): 1514–1516.
[3] Characterization of the Most Odor Active Compounds in an American Bourbon Whisky by Application of the Aroma Extract Dilution Analysis". J. Agric. Food Chem 56 (14): 5813–5819.
[4] Comparison of Aroma Active Volatiles in Oolong Tea Infusions Using GC Olfactometry, GC-FPD and GCMS. J Agric Food Chem. 2015 Sep 2;63 (34):7499510.
[5] Buttery, R. G., Teranishi, R. & Ling, L. C., 1988. Identification of damascenone in tomato volatiles. Chem. Industr. (London), 238.
[6] Guth, H., 1997. Quantification and sensory studies of character impact odorants of different white wine varieties. J. Agric. Food Chem. 45, 3027-3032.
[7] Hartmann, P. J., McNair, H. M. & Zoecklein, B. W., 2002. Measurement of 3-alkyl-2-methoxypyrazine by headspace solid-phase microextraction in spiked model wines. Am. J. Enol. Vitic. 53, 285-288.
[8] Kotseridis, Y. & Baumes, R., 2000. Identification of impact odorants in Bordeaux red grape juice, in the commercial yeast used for its fermentation, and in the produced wine. J. Agric. Food Chem. 48, 400-406.
[9] W. Kohn, L.J. Sham, Phys. Rev. 140 (1965) A1133.
[10] W. Kohn, L.J. Sham, Phys. Rev. 140 (1965) A1133.
[11] C. Lee, W. Yang, R.G. Parr, Phys. Rev. B37 (1988) 785.
[12] B. Miehlich, A. Savin, H. Stoll, H. Preuss, Chem. Phys. Lett. 157 (1989) 200.
[13] Gaussian 03, Revision C.01, M.J. Frisch, G.W. Trucks, H.B. Schlegel, G.E. Scuseria, M.A. Robb, J.R. Cheeseman, J.A. Montgomery, Jr., T. Vreven, K.N. Kudin, J.C. Burant, J.M. Millam, S.S. Iyengar, J. Tomasi, V. Barone, B. Mennucci, M. Cossi, G. Scalmani, N. Rega, G.A. Petersson, H. Nakatsuji, M. Hada, M. Ehara, K. Toyota, R. Fukuda, J. Hasegawa, M. Ishida, T. Nakajima, Y. Honda, O. Kitao, H. Nakai, M. Klene, X. Li, J.E. Knox, H.P. Hratchian, J.B. Cross, C. Adamo, J. Jaramillo, R. Gomperts, R.E. Stratmann, O. Yazyev, A.J. Austin, R. Cammi, C. Pomelli, J.W. Ochterski, P.Y. Ayala, K. Morokuma, G.A. Voth, P. Salvador, J.J. Dannenberg, V.G. Zakrzewski, S. Dapprich, A.D. Daniels, M.C. Strain, O. Farkas, D.K. Malick, A.D. Rabuck, K. Raghavachari, J.B. Foresman, J.V. Ortiz, Q. Cui, A.G. Baboul, S. Clifford, J. Cioslowski, B.B. Stefanov, G. Liu, A. Liashenko, P. Piskorz, I. Komaromi, R.L. Martin, D.J. Fox, T. Keith, M.A. Al-Laham, C.Y. Peng, A. Nanayakkara, M. Challacombe, P.M.W. Gill, B. Johnson, W. Chen, M.W. Wong, C. Gonzalez, J.A. Pople, Gaussian, Inc., Wallingford CT, 2004.
[14] A.P. Scott, L. Random, J. Phys. Chem. 100 (1996) 16502.
[15] R. Dennington, T. Keith, J. Millam, K. Eppinnett, W.L. Hovell, R. Gilliland, GaussView, Version 3.07, Semichem, Inc., Shawnee Mission, KS, 2003.
[16] M.H. Jamroz, Vibrational Energy Distribution Analysis: VEDA 4 Program, Warsaw, 2004.
[17] Mark Ladd, Introduction to Physical Chemistry, third ed., Cambridge University Press, 1998 (Chapter 6).
[18] F.H. Allen, O. Kennard, D.G. Watson, J. Chem. Soc. Perkin Trans. 2 (1987). 12, S1.

ISSN: 2454-1907
DOI: 10.5281/zenodo.1051048

[19] I. Fleming, Frontier Orbitals and Organic Chemical Reactions, John Wiley and Sons, New York, 1976.
[20] A.P. Scott, L. Random, J. Phys. Chem. 100 (1996) 16502.
[21] P. Pulay, G. Fogarasi, G. Pongor, J.E. Boggs, A. Vargha, J. Am. Chem. Soc. 105 (1983) 7037.

*Corresponding author.
E-mail address: akgkp25@ yahoo.co.in